Письма в ЭЧАЯ. 2016. Т. 13, № 1(199). С. 180–189

DEVELOPMENT OF "ACTIVE CORRELATION" TECHNIQUE

Yu. S. Tsyganov [1]

Joint Institute for Nuclear Research, Dubna

With reaching extremely high intensities of heavy-ion beams, new requirements for the detection system of the Dubna Gas-Filled Recoil Separator (DGFRS, FLNR) will definitely be set. One of the challenges is how to apply the method of "active correlations" to suppress the beam associated background products without significant losses in the whole long-term experiment efficiency value. Different scenarios and equations to develop the method according to this requirement are under consideration in the present paper. The execution time to estimate the dead-time parameter associated with the optimal choice of the life-time parameter is presented.

При достижении сверхвысоких интенсивностей пучков тяжелых ионов возникают новые требования к детектирующей системе дубненского газонаполненного сепаратора ядер отдачи (ГНС, ЛЯР). Одна из тем работы — применение метода «активных корреляций» для радикального подавления фона, связанного с пучком циклотрона, без существенных потерь общей эффективности эксперимента. Рассматриваются подходы и уравнения для реализации и развития метода. Представлены оценки дополнительного мертвого времени, связанного с реализацией описанного в работе подхода по определению параметра оптимального времени жизни.

PACS: 27.90.+b; 25.70.-z; 25.75.-q

INTRODUCTION

Significant success has recently been achieved in the field of SHE synthesis and studies of radioactive properties of superheavy nuclei. With the discovery of the "island of stability" [1] in experiments with ^{48}Ca projectiles at the Dubna Gas-Filled Recoil Separator, one can raise a question about sources and components of such a great event. Intense heavy-ion beams and exotic actinide target materials were certainly strongly required in experiments. However, final products of the DGFRS experiments were rare sequences of decaying nuclei signals. In this connection, the role of the DGFRS detection system was crucial. Specifics of the DGFRS detection system is the application of the "active correlation" method [2–4]. Using this technique, it has become possible to provide deep suppression of background products with negligible losses in the value of the whole experimental efficiency. Moreover, experiments at the DGFRS, when the above-mentioned method was not applied, yielded ambiguous results [5–7]. To briefly clarify the method application, the process block diagram is shown in Fig. 1. A short beam stop was generated by the EVR–α sequence detected in real-time mode. Extra time which is required for one-cycle searching is shown in Fig. 2 (i3-2100 CPU@3.10 GHz).

[1] E-mail: tyra@jinr.ru

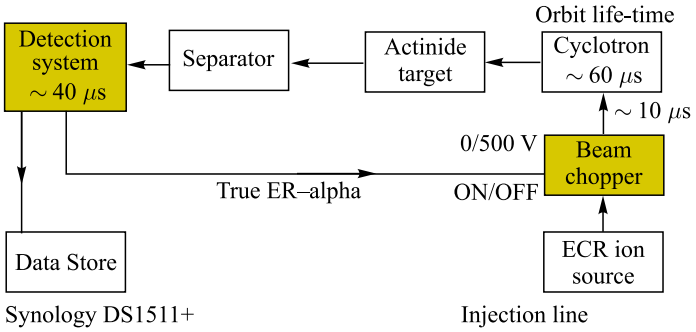

Fig. 1 (color online). Block diagram of the real-time process. Two key elements are shown in yellow color

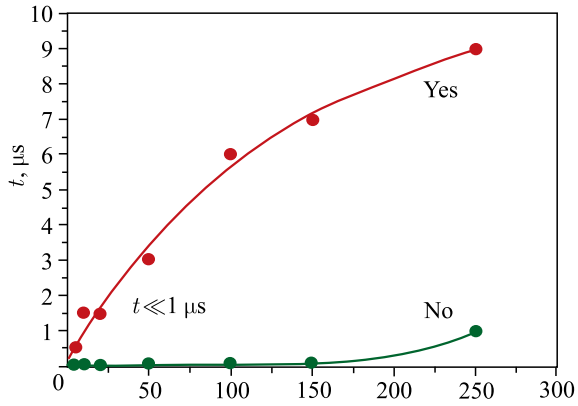

Fig. 2. Extra time $t \ll 1$ μs which is required ($n = 1$ is actual) to search for ER–alpha correlation (scenario Yes)

Note that in most of the DGFRS experiments one of the two first alpha particle signals was used as a trigger signal for a break point in target irradiation.

It is evident that application of the "active correlation" method will cause more than usual break points in continuous, long-term actinide target irradiation and, therefore, will result in additional losses in the experimental efficiency. Without any modification of the method, the loss value may reach tens of percents ($\sim$5–10 pμA intensity), which does not definitely contribute to success in challenging experiments which require a lot of resources. One should note that there are other problems related to high-beam intensities, except for detecting. For instance, the development of the rotating actinide target design is one of them. Additionally, this paper completes a series of works aimed at solving issues related to the DGFRS long-term experiment automation.

1. TWO-MATRIX ALGORITHM FOR REAL-TIME SEARCH FOR $\mathrm{EVR}_1(\ldots\mathrm{EVR}_n)$–$\alpha$ SEQUENCES

It will be quite possible with extra high heavy-ion (HI) beam intensities; sequences like EVR_1–(...EVR_n–...)–α will sometimes be quite probable, though with a lower probability

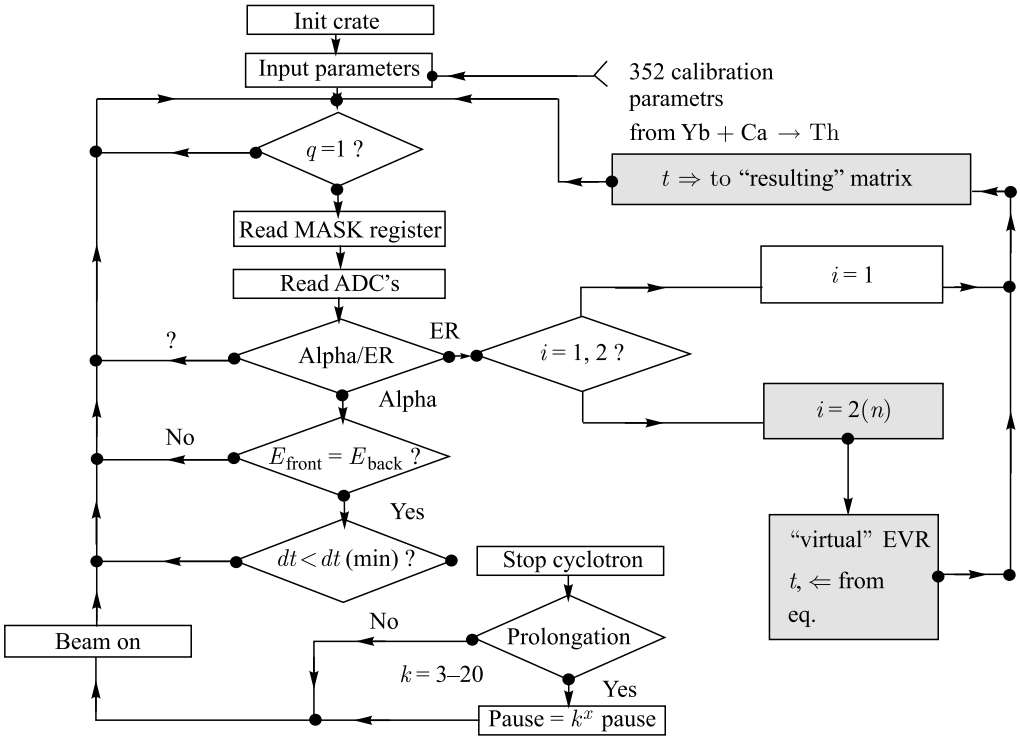

Fig. 3. Flowchart of the modified process. Branch $n > 1$ is in grey color

value than the one for a single EVR–α sequence. Under these circumstances, it seems reasonable, in addition to the standard algorithm [2, 3], to consider two or even more candidates for a starting recoil and thus construct some virtual "effective recoil" in the PC RAM and to consider its time as a registered alpha decay life-time value.

To take into account the above-mentioned scenario, two or even $\forall n\colon\ n > 1$ EVR's matrixes in the PC's RAM are strongly required, except for one matrix in the case of the standard algorithm. In Fig. 3, the flowchart of this process is shown.

In Sec. 2, a general algorithm for the "virtual" recoil signal constructing is presented.

2. METHOD VARIATION FOR THE CASE OF NON-DEFINITE RELATION EVR–α

It was V. B. Zlokazov who first recognized the importance of the theoretical approach to the non-definite mother–daughter nuclei relationship. He epitomized mathematically an equation system to search for an actual life-time value [9].

A more simplified mathematical approach for two candidates for recoil (EVR) was reported in [10] in the form of a transcendental equation relative to the actual life-time parameter. That equation is presented below:

$$\tau = \frac{t_1(1 - \mathrm{e}^{-t_1/\tau}) + t_2(1 - \mathrm{e}^{-t_2/\tau})}{2 - \mathrm{e}^{-t_1/\tau} - \mathrm{e}^{-t_2/\tau}}. \tag{1}$$

Here τ is the actual life-time value; t_1 and t_2 are the measured times between the alpha decay and the first and second recoils, respectively. In [10], using a simple iteration method, a 8-μs time interval was found for 15 iterations, whereas additionally it was established that about a 3-μs (~ 3 iterations; i3-2100 CPU @ 3.10 GHz) time interval satisfied the condition of application of the real-time algorithm aimed at radical suppression of background products associated with the U-400 cyclotron beam.

Nevertheless, one may consider different values for statistical weights of different EVR signals, and sometimes it is useful to extend the above-mentioned equations to a more common case.

a) Let us consider n candidates for the recoil signal and time sequence $t_1, t_2, t_3, \ldots, t_n$, respectively (Fig. 4). Of course, similar to [10], the t_{n+1} signal is as follows: $t_{n+1} \gg t_i$, $i \leqslant n$.

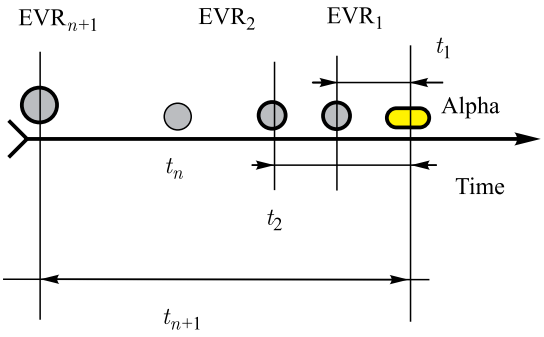

Fig. 4. Scheme of the EVR$_1$–EVR$_2$–. . . –EVR$_n$ $\to \alpha$ sequence. $t_{n+1} \gg t_n$

Following the algorithm described in [10], it is easy to obtain

$$\tau = \frac{\sum\limits_{i=1}^{n} t_1(1 - \mathrm{e}^{-t_i/\tau})}{n - \sum\limits_{i=1}^{n} \mathrm{e}^{-t_i/\tau}}. \tag{2}$$

And with one additional condition[1]:

$$1 - \exp\left(-\frac{t_n}{\langle \tau_{\mathrm{EVR}} \rangle}\right) \ll 1. \tag{2'}$$

In this formula $\langle \tau_{\mathrm{EVR}} \rangle$ is an average time value between two neighbor recoil signals per a pixel. To some extent, one can consider Eqs. (2) and (2′) as a contradiction. So, it is reasonable to consider (2′) as a rough indication to the field of Eq. (2) application if to rewrite (2′) in the form

$$1 - \exp\left(-\frac{t_n}{\langle \tau_{\mathrm{EVR}} \rangle}\right) \approx \varepsilon, \quad \text{where} \quad 0 < \varepsilon < 1^2.$$

b) More exactly to consider a statistical weight parameter taking into account a factor indicating to a pair of EVRs may be a random;

$$\text{that is,} \quad w_i = \frac{1 - \mathrm{e}^{-t_i/\tau}}{1 - \exp\left(-\dfrac{t_i}{\langle \tau_{\mathrm{EVR}} \rangle}\right)}. \tag{3}$$

[1] For the sake of statistical significance.

[2] E.g., $\varepsilon = 0.5$.

c) In the approaches presented above, including [10], similar recoil signals were considered. No difference/divergence was found in energy signal amplitudes registered with the silicon radiation detector. On the contrary, a semi-empirical relationship for the EVR's registered energy value was reported in [11] in the form

$$\langle E_{\rm reg}\rangle \approx -2.05 + 0.73E_{\rm in} + 0.0015E_{\rm in}^2 - \left(\frac{E_{\rm in}}{40}\right)^3. \tag{4}$$

In this equation, $E_{\rm reg}$ is the value of the EVR's signal registered with the PIPS (or DSSSD) silicon radiation detector and $E_{\rm in}$ is the incoming (calculated) EVR's energy value. Taking into consideration the objective of this paper, any deviation from the mean value from (4) for i-recoil ($\forall i \leqslant n$) can be introduced additionally to the w_i value using the standard deviation parameter of the Gaussian distribution shape, as is reported in [12].

The time-of-flight signal value can certainly be considered in the same manner. $\Delta E_{\rm start/stop}$ signals and their distribution (from "start" and "stop" proportional chambers [13, 14]) may also be taken into account. To a first approximation, as TOF/ΔE spectrum distribution is quite wide, one should consider a step-like function for this purpose, namely:

$$\begin{gathered} F({\rm TOF},\Delta E) = 1 : {\rm TOF} \in ({\rm TOF}_{\rm min}, {\rm TOF}_{\rm max})\&\Delta E \in (\Delta E_{\rm min}, \Delta E_{\rm max}), \\ 0 \text{ — all other cases}^1. \end{gathered} \tag{5}$$

Typical shape of ΔE signal spectrum is shown in Fig. 5, *a*.

Gaussian fit of the ΔE signal for (200, 3000) range is shown in Fig. 5, *b*.

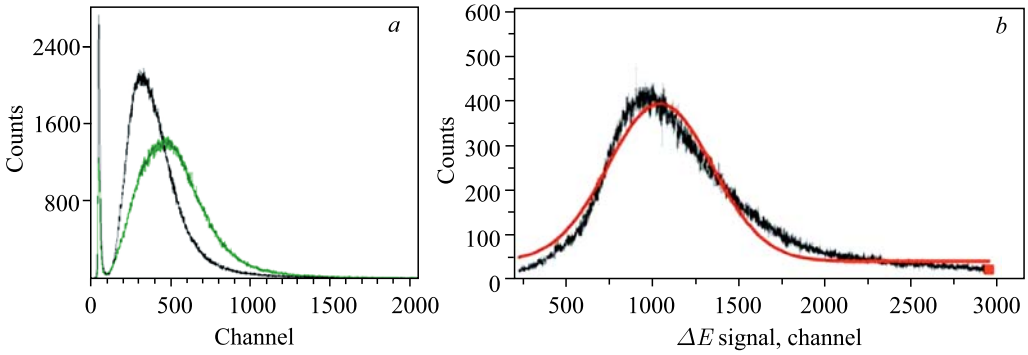

Fig. 5. *a*) Typical shapes for EVR ΔE signals (channels) measured with START and STOP proportional chambers. The pentane pressure value is equal to 1.6 Torr. Both anode biases are equal to +390 V. Both cathode biases are equal to −100 V. Reaction: $^{\rm nat}{\rm Yb} + {}^{48}{\rm Ca} \to {}^{*}{\rm Th}$. *b*) Gaussian fit of the ΔE signal for (200, 3000) range

Therefore, for the case a) the weight function w_i will be as

$$w_i({\rm TOF}_i, \Delta E_i, E_i^{\rm reg}, t_i) = F({\rm TOF}_i, \Delta E_i)(1 - {\rm e}^{-t_i/\tau})\frac{1}{\sigma_i\sqrt{2\pi}}\exp\left(-\frac{\Delta\varepsilon_i^2}{2\sigma_i^2}\right), \tag{6}$$

[1] If necessary, one can take into account more exact approximation, e.g., Poisson-like function.

where the E_i^{reg} value is calculated from (4) and σ_i is a standard deviation, usually of about 2 MeV, and $\Delta\varepsilon_i = E_i^{\mathrm{reg}} - \langle E^{\mathrm{reg}} \rangle$.

d) The case of a few candidates to α-decay is not significant enough to be taken into consideration due to a much lower rate of signals simulating alpha decay in the focal plane detector of the DGFRS.

3. EXAMPLE OF EQUATION (1) SOLUTION FOR $n = 2$

In Fig. 6, *a, b*, a ten-step simple iteration process for the parameter $\Delta = \dfrac{t_2 - t_1}{\tau} = 0.2$ and the initial approximation $x_0 = 0.3$ are shown. Note that although the total execution time is equal to 6 μs, the 1.2-μs interval (two steps) meets the requirements and fulfils the conditions of perfect application of the real-time technique. Note that Newton's method gives nearly the same convergence time in comparison with the simple iteration one.

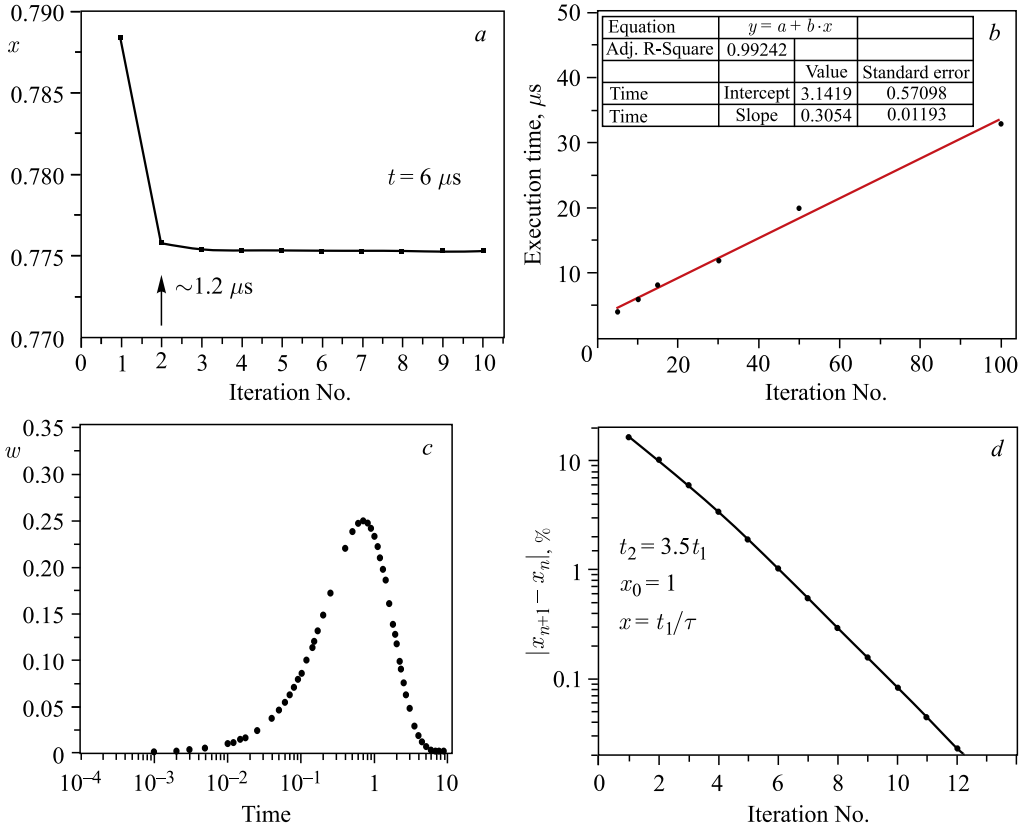

Fig. 6. *a*) Solution of Eq. (1) vs. the number of simple iterations. $x = t_1/\tau$. *b*) Dependence of execution time vs. iteration number. *c, d*) Process of convergence (*d*) of sequence $s_n = |x_{n+1} - x_n|$ for a statistical weight of $w_i \approx \mathrm{e}^{-t_i/\tau}(1 - \mathrm{e}^{-t_i/\tau})n = 2$ (*c*). Note that satisfactory results in the sequence s_n convergence are achieved with $\tau_0 \approx \sqrt[2]{t_1 t_2}$ value taken as a first approximation

4. APPLICATION OF THE COMBINED METHOD

The author has not excluded the combined (relatively recoil signal) method application.

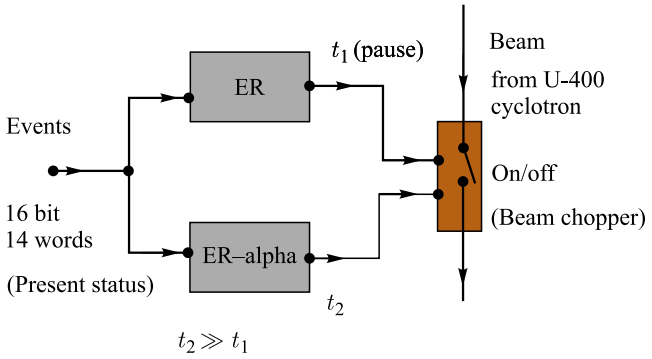

Fig. 7. Scheme of the combined beam-stop real-time algorithm

In other words, when detecting a recoil signal, a shorter beam-off interval is generated by the DGFRS detection system. This trivial algorithm could obviously operate in parallel with the main one ("OR" principle), as is shown in Fig. 7.

5. SUMMARY

Together with conservative approaches minimizing beam associated backgrounds, such as the construction of new electromagnetic recoil separators, fast chemistry, and design of a more perfect silicon radiation detector, the development of the "active correlation" method will definitely contribute to this aim. Moreover, this method will provide radical suppression of background products. The extension of the method is presented above and will undergo exhaustive beam tests in the nearest future.

Of course, the development of new gas-filled recoil separators will contribute to the problem of background suppression too.

Acknowledgements. The author is grateful to Drs. A. Kuznetsov and A. Voinov for their help in some test measurements for this paper. The paper is supported in part by the RFBR Grant No. 13-02-12052.

Appendix
A FEW WORDS ABOUT BASIC ELECTRONICS MODULE IMPLEMENTATION

The first approach to the DGFRS spectrometer implementation was discussed in detail in [8]. This solution is based on a single 16^{in} 12-bit ADC-16 with about 1 μs conversion time [8] and a special digital unit used to obtain the address of the back strip number of the DSSSD detector. Consequently, the description of the C++ code reported in [8] is outside the scope of the present paper. Another reasonable scenario is based on the application of the universal CAMAC 1M 16^{in} amplifier-multiplexer-ADC integrated module ADP-16 produced

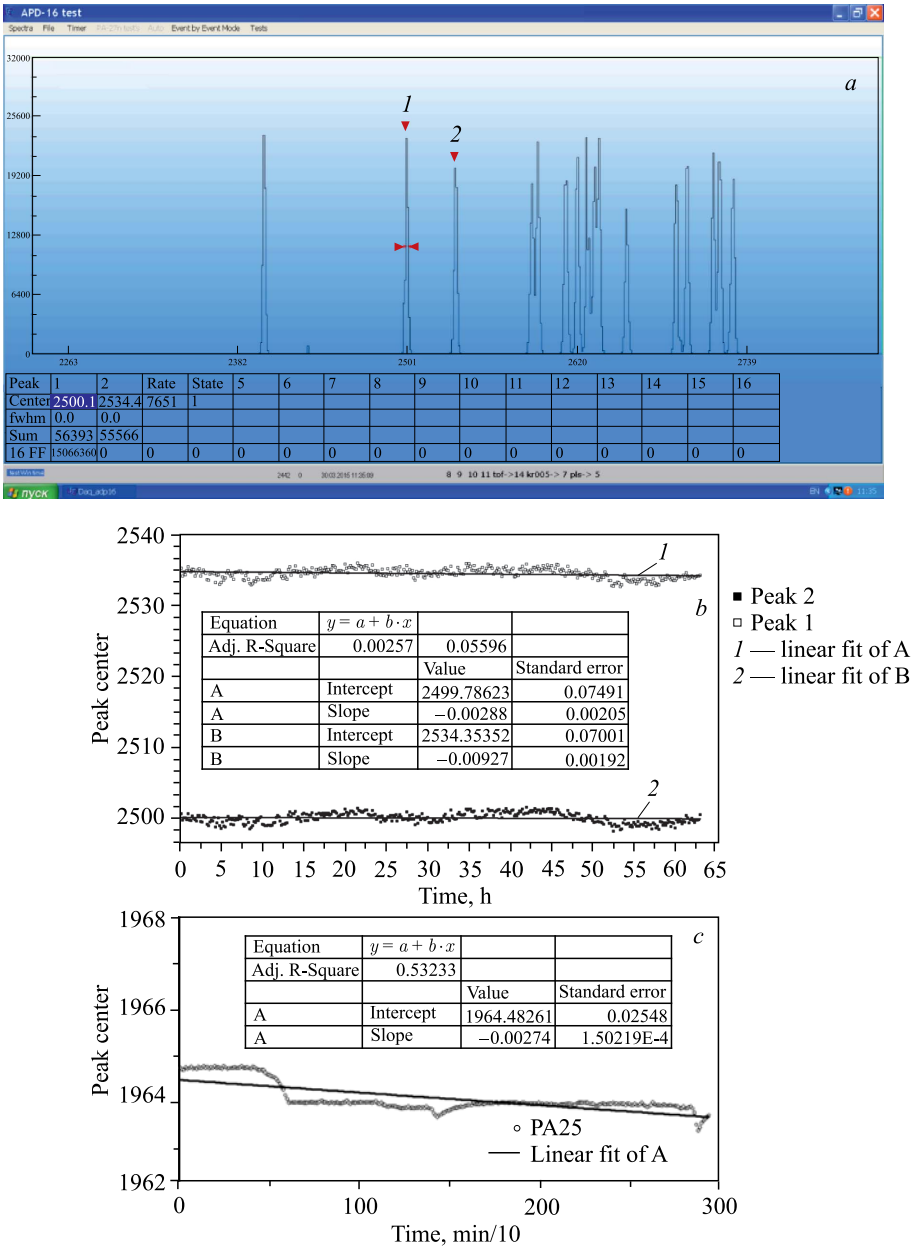

Fig. 8. *a*) Test spectra from IMI2011-ADP-16. The bottom line of the table in the figure shows event number per each channel. Peaks 1 and 2 of the stability test are shown by the triangles. *b*) Stability test for ADP-16 (left peak in 8, *a*). Linear fit results are presented in the table within. The standard deviation value is equal to 0.07 channels for both peaks. With using special design thermostabilized resistors the whole stability will be more perfect. *c*) Stability test for ADC PA-25. Standard deviation is equal to 0.025 channels

by TekhInvest Dubna [16]. Below the author is reporting the results of a preliminary test of the first TekhInvest module using the IMI2011 special purpose generator module[1] [14]. To carry out the test, the author designed the Builder C++ (Windows) code. The mentioned module has a capability to store eight signal amplitudes together with their synchronized times in the internal buffer memory. It allows detection of short (~ 2.5 μs) sequences of signals. Therefore, the signal sequences of $x_1 \to x_2 \to \ldots x_n : n \leqslant 8 : 0 \to 2.5$ μs $\to 2.5 \to n\tau_{\mathrm{dead}}$ (writing time–reading time) will be successfully detected with their time stamps with the microsecond accuracy. Here, τ_{dead} is the regular dead-time value of the spectrometer. The τ_{dead} value depends on the actual spectrometer crate configuration (the number of actual stations and their CAMAC functions in use). The tested module has the following CAMAC functions:

— N*A(0)[F(0)+F(2)] alpha particle scale reading (13 bit);
— N*A(1)[F(0)+F(2)] fission fragment (heavy-ion) scale reading (12 bit);
— N*A(2)[F(0)+F(2)] synchronized time (in μs) reading;
— N*A(0)*F(8) test LAM;
— N*A(0)*F(10) data reset;
— N*A(0)*F(16) W(8...1) threshold setting;
— N*A(0)*F(24) masking L;
— N*A(0)*F(26) de-masking L.

In Fig. 8, *a, b*, test spectra are shown in the right part of the main window. FF-scale spectrum is shown in the upper left corner. Additionally, one general conclusion can be drawn here: the prototype of new Builder C++ based software for the DGFRS has been successfully tested.

REFERENCES

1. *Oganessian Yu. Ts., Utyonkov V. K.* Superheavy Element Research // Rep. Prog. Phys. 2015 (in press).
2. *Tsyganov Yu. S., Polyakov A. N., Sukhov A. N.* An Improved Real-Time PC Based Algorithm for Extraction of Recoil–Alpha Sequences in Heavy-Ion Induced Nuclear Reactions // Nucl. Instr. Meth. A. 2003. V. 513. P. 413–416.
3. *Tsyganov Yu. S., Polyakov A. N.* Real-Time Operating Mode with DSSSD Detector to Search for Short Correlation ER–Alpha Chains // Cybernetics Phys. 2014. V. 3, No. 2. P. 85–90.
4. *Tsyganov Yu. S.* Method of "Active Correlations" for DSSSD Detector Application // Phys. Part. Nucl. Lett. 2015. V. 12, No. 1. P. 83–88.
5. *Oganessian Yu. Ts. et al.* The Synthesis of Superheavy Nuclei in the $^{48}\mathrm{Ca} + {}^{244}\mathrm{Pu}$ Reaction // Revista Mexicana de Fisica. 2000. V. 46. Suppl. 1. P. 35–41.
6. *Lazarev Yu. A. et al.* α-Decay of $^{273}110$: Shell Closure at $N = 162$ // Phys. Rev. C. 1996. V. 54, No. 2. P. 620–625.
7. *Zlokazov V. B., Tsyganov Yu. S.* Half-Life Estimation under Indefinite "Mother–Daughter" Relation // Phys. Part. Nucl. Lett. 2010. V. 7, No. 6. P. 401–405.
8. *Tsyganov Yu. S.* Elements of Automation of the DGFRS Experiments // Part. Nucl., Lett. 2015. V. 12, No. 1(192). P. 116–127.

[1]The module generates 16 channels of signals similar to the ones from the spectroscopy shape amplifier.

9. *Tsyganov Yu. S.* Synthesis of New Superheavy Elements at the DGFRS: Complex of Technologies // Phys. Part. Nucl. 2014. V. 45, No. 5–6. P. 817.
10. *Tsyganov Yu. S.* Parameter of Equilibrium Charge States Distribution Width for Calculation of Heavy Recoil Spectra // Nucl. Instr. Meth. A. 1996. V. 378. P. 356–359.
11. *Mezentsev A. N. et al.* Low Pressure TOF Module // FLNR (JINR) Sci. Report 1992–1993. Dubna, 1993. P. 203.
12. *Tsyganov Yu. S. et al.* Focal Plane Detector of the Dubna Gas-Filled Recoil Separator // Nucl. Instr. Meth. A. 1997. V. 392. P. 197–201.
13. *Tsyganov Yu. S.* A New Reasonable Scenario to Search for ER–Alpha Energy-Time-Position Correlated Sequences in a Real Time Mode // Phys. Part. Nucl. Lett. 2015. V. 12, No. 4. P. 885–894.
14. *Tsyganov Yu. S.* ADP-16 1M Module, IMI2011 Module // Proc. of NEC'2015 Intern. Symp., Budva, Montenegro, Sept. 26 – Oct. 02, 2015 (in press).

Received on April 29, 2015.